Environmental Science & Technology

Article

pubs.acs.org/est

Biochar and Microbial Signaling: Production Conditions Determine Effects on Microbial Communication

Caroline A. Masiello,*[,†] Ye Chen,[‡] Xiaodong Gao,[†] Shirley Liu,[‡] Hsiao-Ying Cheng,[§] Matthew R. Bennett,[‡] Jennifer A. Rudgers,[⊥] Daniel S. Wagner,[‡] Kyriacos Zygourakis,[¶] and Jonathan J. Silberg*[,‡,§]

[†]Department of Earth Science, [‡]Department of Biochemistry and Cell Biology, [§]Department of Bioengineering, and [¶]Department of Chemical and Biomolecular Engineering, Rice University, 6100 Main Street, Houston, Texas 77005, United States

[⊥]Department of Biology, University of New Mexico, 167 Castetter Hall, Albuquerque, New Mexico 87131, United States

Supporting Information

ABSTRACT: Charcoal has a long soil residence time, which has resulted in its production and use as a carbon sequestration technique (biochar). A range of biological effects can be triggered by soil biochar that can positively and negatively influence carbon storage, such as changing the decomposition rate of organic matter and altering plant biomass production. Sorption of cellular signals has been hypothesized to underlie some of these effects, but it remains unknown whether the binding of biochemical signals occurs, and if so, on time scales relevant to microbial growth and communication. We examined biochar sorption of *N*-3-oxo-dodecanoyl-L-homoserine lactone, an acyl-homoserine lactone (AHL) intercellular signaling molecule used by many gram-negative soil microbes to regulate gene expression. We show that wood biochars disrupt communication within a growing multicellular system that is made up of sender cells that synthesize AHL and receiver cells that express green fluorescent protein in response to an AHL signal. However, biochar inhibition of AHL-mediated cell−cell communication varied, with the biochar prepared at 700 °C (surface area of 301 m^2/g) inhibiting cellular communication 10-fold more than an equivalent mass of biochar prepared at 300 °C (surface area of 3 m^2/g). These findings provide the first direct evidence that biochars elicit a range of effects on gene expression dependent on intercellular signaling, implicating the method of biochar preparation as a parameter that could be tuned to regulate microbial-dependent soil processes, like nitrogen fixation and pest attack of root crops.

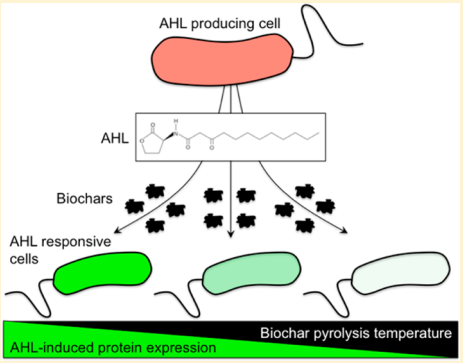

INTRODUCTION

Charcoal is a ubiquitous component of the Earth system, present not only in the soils of fire-affected ecosystems, but also in marine sediments and terrestrial and marine dissolved organic carbon pools.[1] It also forms the basis for a form of carbon sequestration called soil biochar amendment,[2] where charcoal is intentionally added to soil with the aim of increasing the size of the stable organic carbon pool while potentially delivering other agronomic benefits such as increased crop productivity,[1,3−5] decreased soil tensile strength,[2,6] altered soil water properties,[7−10] improved plant pest resistance,[11] and decreased nitrogen loss from soils.[12] The carbon sequestration potential of biochar is based on the assumption that a large fraction of this material is an inert component of the soil organic matter pool with a very long soil residence time.[13] Large-scale data on the biogeochemical cycling of charcoal back up the idea that it decomposes slowly in the Earth system,[14,15] and laboratory and ecosystem studies are narrowing down the factors that control charcoal soil residence time.[16−20]

As commercial applications of biochar have begun, results have appeared which challenge the inert nature of this material and suggest more complex carbon cycle roles. For example, biochar addition to soil has been shown to promote the loss of noncharcoal organic matter (priming) in some studies,[21] but not in others.[22] This priming of soil decomposition causes an enhanced flux of CO_2 into the atmosphere from soils, potentially decreasing the carbon sequestration benefits of biochar, as well as decreasing ecosystem services provided by soil organic matter. Other evidence has appeared suggesting that biochar can enhance retention of nitrogen molecules that contribute to soil fertility,[23,24] stimulate colonization of roots by mycorrhizal fungi,[25,26] change soil microbial composition,[27] and confer plant resistance to microbial pathogens.[28] These biological effects have been proposed to arise in part because biochars sorb diffusible small molecules that soil organisms use for intercellular communication and coordinated decision-making.[25,29] Biochars are known to bind diverse organic molecules,[30] many of which are nonpolar like the molecules used for intercellular communication. Numerous studies have analyzed the kinetics

Received: April 3, 2013
Revised: September 5, 2013
Accepted: September 11, 2013
Published: September 11, 2013

of biochar sorption to organics on time scales (days to months) relevant to the mobilization of pollutants.[29,31−33] However, it remains unclear if communication can be altered by the presence of biochars on the time scales of microbial signaling and gene expression (minutes to hours).

It is challenging to directly demonstrate biochar-driven mechanisms for observed biological effects within the environment because of the complexity and diversity of conversations occurring among microbes and plants. Bacteria communicate with one another using a variety of biochemicals,[34] which are distinct from the molecules used by fungi for intraspecies communication.[35] Plants also synthesize flavinoids that regulate microbial behaviors, such as the establishment of root nodules,[36] and microbes synthesize nodulation signals[37] and plant hormones[38] that influence plant development and nutrient uptake. The diversity of signals present in the environment creates challenges in attributing causality to any particular intercellular conservation. The high light absorptivity of biochar and soils adds to this challenge. While there exist microbial biosensors capable of synthesizing reporters that can be imaged when they encounter biological signals within the rhizosphere,[39,40] fluorescent reporters tend to absorb and emit light in a visible range that is unsuitable for imaging cells within biochar-amended materials, which have high light absorption.

To better understand the effects of biochars on cellular communication, we investigated how biochar materials created under different pyrolysis temperatures (300, 350, 400, 450, 550, 600, and 700 °C) influence signal detection within a synthetic microbial system.[41] Because the relevant question is the detectability of molecular signals by microbes (as opposed to the chemically extractable fraction of signal present in the soil), we used a microbial sensor to determine when signaling molecules fell below a level detectable to bacteria in the presence of different biochars. We focused our attention on *N*-3-oxo-dodecanoyl-L-homoserine lactone, a member of the acyl-homoserine lactone (AHL) signaling molecule family that are used for intraspecies communication and quorum sensing by many gram-negative bacteria, including nitrogen fixing plant symbionts and pathogens that cause soft rot in plants.[42,43]

MATERIALS AND METHODS

Materials. *Escherichia coli* XL1-Blue were from Stratagene, and *E. coli* BLIM cells were kindly provided by K. S. Matthews.[44] The acylhomoserine lactone (AHL) used, *N*-3-oxo-dodecanoyl-L-homoserine lactone, was from Cayman Chemical, bacterial growth media components were from BD Biosciences, and all other reagents were from Sigma-Aldrich and VWR.

Biochar Synthesis. Slow pyrolysis of *Prosopis glandulosa* (mesquite) wood to generate biochar was performed using a fixed bed reactor as described previously.[7] In brief, mesquite feedstocks ground to 20 mesh (<0.853 mm) were placed in a stainless steel crucible, which was then plugged with ceramic wool, capped with a ceramic bowl, and buried in fine-grained quartz sand inside a larger, open-top stainless steel crucible. This reactor system was heated in a muffle furnace at 5 °C min^{-1} to the desired reaction temperatures (300, 350, 400, 450, 550, 600, and 700 °C) and held at each temperature for 4 h. The products were manually mixed after cooling to increase homogeneity.

Surface Area Measurements. We measured the biochar surface area using a Quantachrome Autosorb-3b Surface Analyzer. Prior to analysis, samples were placed in ashed (550 °C for 4 h) glass cells and vacuum-dried overnight at 200 °C. Nitrogen adsorption/desorption isotherms were obtained at 77 K by a 26-point analysis for relative pressures P/P_0 from 1.21×10^{-4} to 0.99, where P is the adsorption equilibrium pressure and P_0 is the vapor pressure of bulk liquid N_2 at the experimental temperature. Specific surface area was calculated using Brunauer−Emmett−Teller (BET) theory.[45]

Receiver Plasmids. Receiver plasmids contained the synthetic P_{lasR} promoter fused to a strong RBS (BBa_B0034) and GFP gene (BBa_E0040) from the IGEM registry. These plasmids additionally contained a pMB1 origin from pET28a and either a chloramphenicol (Cm^R) or a kanamycin (Kan^R) selectable marker.

Sender Plasmid. The sender plasmid contained the $P_{A1lacO-1}$ promoter[46] fused to a strong RBS and a gene fusion that was made up of the LasI gene (BBa_C0078) fused to the mCherry gene through a $(GGGGS)_3$ peptide linker. This plasmid additionally contained a pMB1 origin, a Cm^R marker, and the LacI gene from pET28a. In this sender plasmid, the *N*-3-oxo-dodecanoyl-L-homoserine lactone synthase gene, LasI, is expressed as a fusion to mCherry through a $(GGGGS)_3$ linker using a $P_{A1lacO-1}$ promoter, which is constitutively active in cells that lack the repressor LacI, such as *E. coli* BLIM cells.[44] The function of this fusion protein is indistinguishable from LasI.

Effect of AHL on GFP Expression in Liquid Culture. *E. coli* XL1 Blue harboring the receiver plasmid (Cm^R) were grown to stationary phase in LB medium containing 34 μg/mL chloramphenicol, diluted to an A_{600} = 0.05 in 50% LB medium that contained varying concentrations of AHL (0, 5, 25, 50, 125, 250, 500, 1000, and 2000 nM), and grown to stationary phase at 30 °C. GFP levels were determined by measuring whole cell fluorescence emission (509 nm) upon excitation of 488 nm using a Tecan M1000 plate reader. Fluorescence was normalized to culture absorbance at 600 nm to account for variability in growth.

Effect of Biochar on AHL Availability in Water. Varying concentrations of each biochar (1, 5, 10, 25, and 50 mg/mL) prepared at different temperatures (300, 350, 400, 450, 550, 600, and 700 °C) were incubated with 1 μM AHL within water for 6, 60, or 1440 min. After incubation, biochar was removed through centrifugation (14 000*g* for 1 min), and 100 μL of the soluble fraction was mixed with an equal volume of LB medium containing *E. coli* transformed with the Cm^R receiver plasmid at an OD_{600} = 0.05 and 50 μg/mL chloramphenicol. This mixture was grown for 18 h within 96-well microtiter plates incubated at 30 °C and shaken at 250 rpm. Green cellular fluorescence (λ_{ex} = 488; λ_{em} = 509) and absorbance (600 nm) were measured using 200 μL of each culture after growing cells in a shaking incubator (30 °C; 250 rpm) for 18 h. To account for variation in cell density, fluorescence to absorbance ratio was calculated for each well, and the calculated values were normalized to those observed with cells that were grown in the absence of AHL and in the presence of AHL that was not incubated with a biochar.

Effect of Colony Separation on Intercellular Signaling. *E. coli* XL1 Blue harboring the Kan^R receiver plasmid and *E. coli* BLIM transformed with the Cm^R sender plasmid were grown to stationary phase in LB containing 50 μg/mL kanamycin and 50 μg/mL chloramphenicol, respectively. Bacteria (1 mL) were harvested by centrifugation, washed with 1 mL of 25% glycerol, resuspended in 1 mL of 25% glycerol, and diluted 10-fold in 25% glycerol. Resuspended receiver (8 μL) and sender cells (3 μL) were spotted at different distances (1, 10, 20, and 30 mm) from one another on 1.5% agar plates containing M9 minimal medium and 20 amino acids. A smaller volume of the sender strain was spotted to avoid growth of these cells over the biochar agar slabs during the overnight incubation. Spotting was performed in

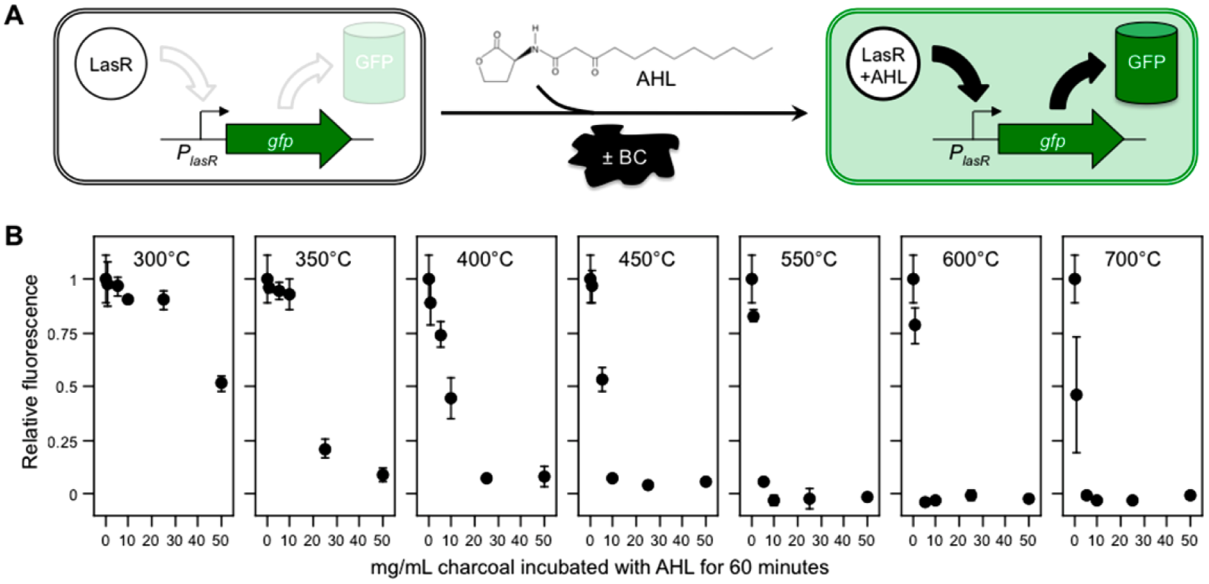

Figure 1. Sorption of AHL by biochars pyrolyzed over a range of temperatures. (A) *E. coli* transformed with the receiver plasmid synthesize GFP when grown in an environment containing the AHL *N*-3-oxo-dodecanoyl-L-homoserine lactone. The transcriptional activator LasR, which is constitutively expressed from this plasmid, turns on transcription of the GFP gene upon binding AHL. (B) Effect of biochar-treated AHL on GFP expression within *E. coli* harboring the receiver plasmid. Varying concentrations of biochar were incubated with AHL for 1 h prior to adding the soluble fraction to cells harboring the receiver plasmid. Cells were grown 18 h to allow for AHL-induced GFP expression, which was normalized to the value observed when cells were grown in the presence of untreated AHL. All measurements were performed in triplicate and are reported as the mean ±1 standard deviation. Biochar is designated BC in the figure.

triplicate at each separation distance. After spotting, plates were incubated overnight at 37 °C and then photographed with a Canon Digital Rebel mounted on a Leica MZFLIII microscope at 0.4× magnification with white light (5 ms exposure), a Chroma 41012 GFP long pass filter set (200 and 500 ms exposures), and a Chroma 11002 Green filter (200 and 500 ms exposures). The image analysis software ImageJ was used to quantify the fluorescence from receiver colonies on each agar plate.[47]

Effect of Biochar on Cell−Cell Communication on Solid Medium. Agar plates for assessing cellular communication were prepared by placing a mold (sterilized through immersion in ethanol) within sterile polystyrene plates (60 × 15 mm) and pouring 8 mL of 1.5% agar containing M9 medium and 20 amino acids. Upon cooling the mold was removed to leave a pair of empty adjacent wells. The left well (control) on each plate was filled with 1 mL of liquid agar (1.5%) dissolved in water (65 °C). The right well (experimental) was then filled with 1 mL of liquid agar containing or lacking 10 mg of 300 or 700 °C biochar. *E. coli* XL1 Blue harboring the Kan^R receiver plasmid and *E. coli* BLIM transformed with the Cm^R sender plasmid were grown to stationary phase in LB containing 50 μg/mL kanamycin and 50 μg/mL chloramphenicol. Bacteria were harvested by centrifugation, washed with 25% glycerol, resuspended in 25% glycerol, and diluted 10-fold into 25% glycerol. The 10-fold dilution of sender cells (3 μL) was spotted between the two agar slabs on plates, whereas the 10-fold dilution of receiver cells (8 μL) was spotted on the outside of each agar slab. After spotting, plates were incubated overnight at 37 °C and then photographed with a Canon Digital Rebel on a Leica MZFLIII microscope at 0.4× magnification with white light (5 ms exposure), a Chroma 41012 GFP long pass filter set (200 and 500 ms exposures), and a Chroma 11002 Green filter (200 and 500 ms exposures). ImageJ was used to quantify the fluorescence from the pair of receiver colonies on each agar plate. The ratio of the signals from the pair of receiver colonies on each plate was calculated (receiver adjacent to biochar/receiver adjacent to empty agar) to determine the level of signal inhibition elicited by each biochar. All measurements were performed in triplicate, and values reported represent the average of three independent experiments $\pm 1\sigma$.

Calculating the Effect of Biochar on AHL Diffusion. To estimate the effect of biochar on AHL diffusion within agar plates, the effective diffusion coefficient D_e of AHL was calculated as $(1 - \varepsilon)D_0/[1 - 0.5 \ln(1 - \varepsilon)]$, where D_0 is the actual diffusion coefficient in biochar-free agar medium and ε is the volume fraction occupied by biochar particles in the agar-biochar cube.[48] This analysis revealed that the low volume fraction used in our experiments (less than 2% v/v biochar) decreases the AHL diffusion constant by less than 3%. This implicates sorption as the major mechanism responsible for biochar effects on sender−receiver cell−cell signaling.

RESULTS AND DISCUSSION

Autoinducer Sorption to Biochars. To assay whether biochars influence the availability of AHLs, we constructed a bacterial biosensor[39] that expresses a green fluorescent protein (GFP) reporter when bacterial cells encounter the AHL *N*-3-oxo-dodecanoyl-L-homoserine lactone in their local environment. This was accomplished by transforming *E. coli* with a plasmid that (i) constitutively expresses the protein LasR, a *Pseudomonas aeruginosa* AHL-dependent protein that activates transcription from the promoter P_{lasR}, and (ii) expresses GFP under control of the LasR-dependent promoter P_{lasR}. Cells containing this receiver plasmid displayed increased GFP production when they were grown in medium containing AHL (Supporting Information, Figure S1), because LasR requires bound AHL to activate transcription of genes whose expression is regulated by the LasR promoter.[49] We assayed AHL signaling in *E. coli* because this organism does not use AHL to communicate, lacks the complex responses of soil bacteria that are sensitive to

one or more AHL, and does not produce lactonase enzymes that hydrolyze AHL. With this bacterial biosensor, only two parameters determine AHL levels in the medium: the amount of AHL added to the medium and fraction of the AHL that sorbs to biochar.

We produced a suite of biochars by pyrolyzing *Prosopis glandulosa* (mesquite) wood chips over a range of temperatures (300, 350, 400, 450, 550, 600, and 700 °C). N_2 sorption analysis of these biochars revealed surface areas that spanned more than 2 orders of magnitude (Supporting Information, Figure S2). Varying amounts of each biochar (1 to 50 mg/mL) were incubated with a concentration of AHL (1 μM) sufficient to activate *E. coli* to synthesize GFP (Supporting Information, Figure S1). This level of AHL is within a range that is thought to be biologically relevant for *Pseudomonas aeruginosa*.[50] Initial incubations were performed on the time scale of *E. coli* reproduction. After 60 min, the biochar was separated from unbound AHL by centrifugation, the soluble fraction was mixed with a low density culture of *E. coli*, and cells were grown to stationary phase to allow for GFP expression. Whole cell GFP fluorescence measurements revealed that incubation of AHL with the highest concentrations of each biochar decreased AHL-dependent cellular fluorescence in all cases (Figure 1). The concentration of biochar required to suppress cellular fluorescence varied with biochar pyrolysis temperature and surface area. The biochars with similar low surface areas (300, 350, and 400 °C) required the highest concentrations to suppress GFP expression half maximally (10−50 mg/mL), the biochars with the highest surface areas (550, 600, and 700 °C) required the lowest concentrations to suppress GFP expression half maximally (1−2 mg/mL), and the biochar with an intermediate surface area (450 °C) required an intermediate level of biochar (5 mg/mL) to suppress GFP expression half maximally. We also found that the correlation between biochar surface area and the concentration required for half maximal inhibition of GFP fluorescence could be described by a simple exponential model, R^2 = 0.99 (Figure 2). This trend implicates the AHL binding capacity of the biochar as dependent on surface area and pyrolysis temperature under the conditions used to produce our biochars. Cells incubated with biochar-treated AHL all grew to a similar maximal density (Supporting Information, Figure S3), indicating that biochar-treated water did not alter cell growth.

We also sought to establish whether the biochar sorption of AHL had reached equilibrium with our low surface area biochars and whether biochar sorption occurred on an even faster time scale with our high surface area biochars, for example, faster than the doubling time of *E. coli* in rich growth medium. If some biochars sorb AHL on the time scale of very rapidly growing *E. coli* under optimal growth conditions in a lab, they are likely to sorb AHL under the lower nutrient, slower growth conditions experienced by soil microbes in the environment. To address these questions, we varied the incubation time of AHL and biochar prior to mixing the soluble fraction with *E. coli*. Incubation of low temperature biochars (300 to 400 °C) with AHL for 24 h showed a greater inhibition of GFP expression than 1 h incubation (Supporting Information, Figure S4), indicating that these reactions had not reached equilibrium after 1 h. The lack of saturation suggests the ability of biochar to cause a continued suppression of microbial signaling as bacterial populations grow. In addition, AHL-induced cellular fluorescence was suppressed when the high temperature biochars (550−700 °C) were incubated with AHL for only 6 min prior to mixing with *E. coli* (Supporting Information, Figure S5). This

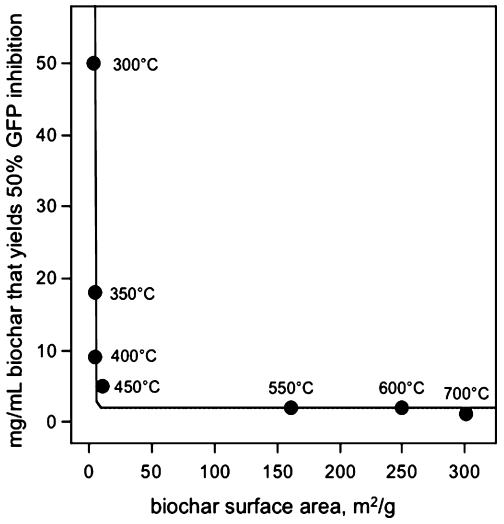

Figure 2. Relationship between biochar surface area, production temperature, and inhibition of GFP reporter expression. The concentration of biochar required to decrease AHL-induced GFP fluorescence by 50% within whole cells was estimated from the data presented in Figure 1 and plotted versus biochar surface area measured using BET analysis. A fit of this data to an exponential model, [biochar] = 1.99 + 2061.9 × exp[−1.38 × (biochar surface area)], yields an R^2 = 0.99.

latter finding suggested that some biochars are capable of adsorbing AHL on the very shortest time scales of microbial reproduction and signaling within rich growth medium, a condition that likely represents the upper bound on the rate of growth and signaling within the environment.

Effect of Biochars on AHL-Mediated Cell−Cell Communication. To directly assess whether biochars can disrupt communication among growing bacteria, we built a sender plasmid that programs *E. coli* to express *P. aeruginosa* LasI (Figure 3A), the acyl-homoserine lactone synthase that continuously synthesizes the AHL *N*-3-oxo-dodecanoyl-L-homoserine lactone from bacterial metabolites.[51] LasI was expressed as a fusion to the red fluorescent protein mCherry to allow for visualization of expression. To make LasI production of *N*-3-oxo-dodecanoyl-L-homoserine lactone continuous within sender cells, we used a $P_{A1lacO-1}$ promoter to constitutively express the LasI-mCherry fusion protein and *E. coli* BLIM cells that are devoid of the transcriptional repressor LacI, which inhibits expression of genes from this promoter. To determine how receiver−sender cell−cell communication varied with distance within a synthetic multicellular system,[41] *E. coli* cells harboring each plasmid type were spotted onto solid growth medium at different edge-to-edge distances from one another (10 to 30 mm), and cell density and GFP expression levels were imaged after overnight growth using visible and fluorescence microscopy, respectively (Figure 3B). Cells harboring each plasmid displayed similar growth under all conditions analyzed. However, the cells containing the receiver plasmid displayed GFP fluorescence that was inversely related to the distance between the sender and receiver cells. When sender and receiver cells were separated by 10 to 20 mm, a gradient of GFP expression was observed within the receiver cells (Figure 3C). While this separation is greater than the distance where signaling is thought to occur on plant surfaces in natural systems,[52] it was necessary for imaging the GFP reporter signal without biochar interference.

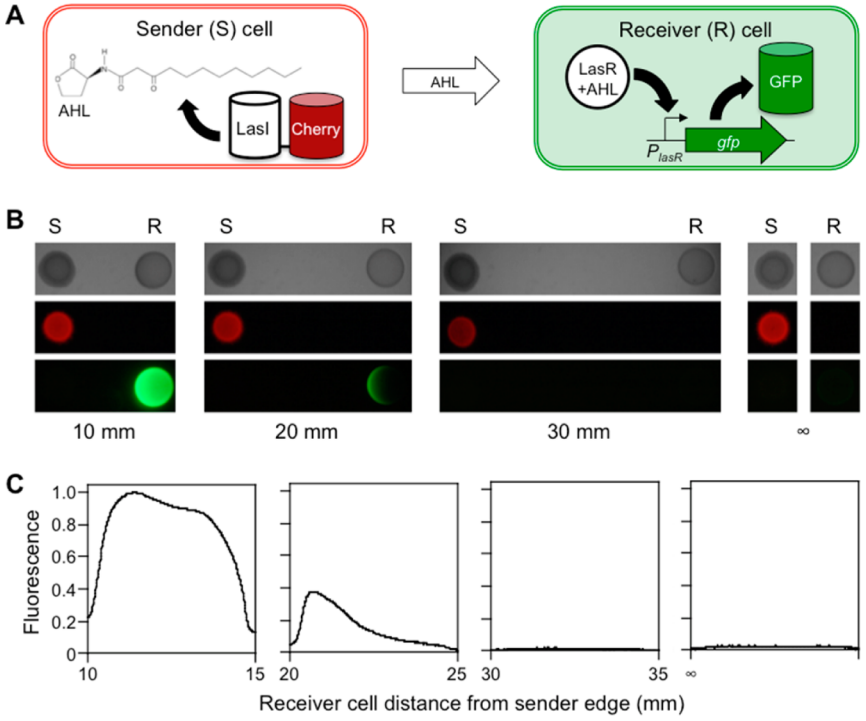

Figure 3. Distance dependence of AHL-mediated cell−cell signaling. (A) Sender *E. coli* constitutively synthesize the AHL *N*-3-oxo-dodecanoyl-L-homoserine lactone, which diffuses into the environment and actives GFP expression when receiver cells are sufficiently proximal. (B) Image of agar plates containing colonies of receiver and sender cells growing at different distances from one another. Bright-field images (top) demonstrate cell health and consistency of growth, red fluorescence images (middle) verify constitutive expression of LasI-mCherry, and green fluorescence images (bottom) show the effect of receiver−sender separation on GFP expression within receiver cells. (C) The green fluorescence across receiver colonies was quantified using ImageJ and normalized to the maximal intensity.

The varying rates of AHL sorption by low and high temperature biochars suggested that the surface area and adsorption capacities of each biochar, which are determined in part by pyrolysis temperature, would influence the extent to which biochars interfere with microbial communication. To test this idea, we examined how signaling between sender and receiver cells growing on agar plates was altered when the AHL signal produced by sender cells had to diffuse through agar containing the biochars that displayed the largest differences in AHL sorption, 300 and 700 °C materials. Since pyrolyzed organic matter strongly absorbs the wavelengths of light used for GFP excitation and emission, we separated sender and receiver cells using a cuboid slab (8 × 37 × 3.4 mm) of the agar medium (1 mL) containing a low concentration (10 mg/mL) of biochar particles (Supporting Information, Figure S6). Biochar occupied only a very small volume fraction (less than 2%) of these agar slabs and should have a negligible effect on the diffusion coefficient of AHL. This arrangement allowed for imaging of GFP expression within receiver cells without biochar interference. To control for signaling variation arising from plate to plate variability in sender cell density, for example, differences in number of sender cells spotted or variability in the temperature experienced within the incubator, signaling through an agar slab lacking biochars was assayed on the same plate by placing a second agar slab and spot of receiver cells on the opposite side of the sender cells (Figure 4A). This allowed us to avoid error associated with this variability by never comparing the fluorescence intensities between individual plates, but instead comparing the relative signals from the two spots of receiver cells on each plate.

Visible images show that receiver cells grew to similar extents when proximal and distal from biochars (Figure 4B), and red fluorescence images reveal constitutive expression of LasI-mCherry within all of the sender cells. These findings show that in this system, biochars did not interfere with bacterial growth or alter gene expression that was not regulated by AHL. However, receiver cells grown adjacent to both low and high temperature biochars displayed decreased green fluorescence compared to cells grown next to empty agar. We quantified the effect of each biochar on cell−cell communication by calculating the ratio of GFP expression within the two spots of receiver cells on each plate (Supporting Information, Figure S7). In the case of the low temperature biochar, the receiver cells adjacent to the biochar exhibited 24.1 ± 2.1% of the GFP fluorescence observed in the receiver cells grown adjacent to agar lacking biochar. In contrast, the receiver cells grown adjacent to high temperature biochar (700 °C) displayed 2.2 ± 1.5% of the GFP fluorescence observed within the receiver cells grown adjacent to empty agar. These findings provide the first direct evidence that biochars are capable of altering protein expression that depends on intercellular signaling, and they show that biochar-induced changes in protein expression can vary by an order of magnitude.

Implications for Biochar Use. We have shown that biochars produced at different temperatures vary in the extent to which they disrupt cell−cell communication among growing bacteria involving one type of AHL. The biochar concentration that elicited this effect (1% by mass) is comparable to the levels that generate biological effects within soils.[5,53] This work has implications for carbon sequestration following biochar amendment to soils. Biochars that interfere with microbial conversations could directly alter soil respiration by changing the

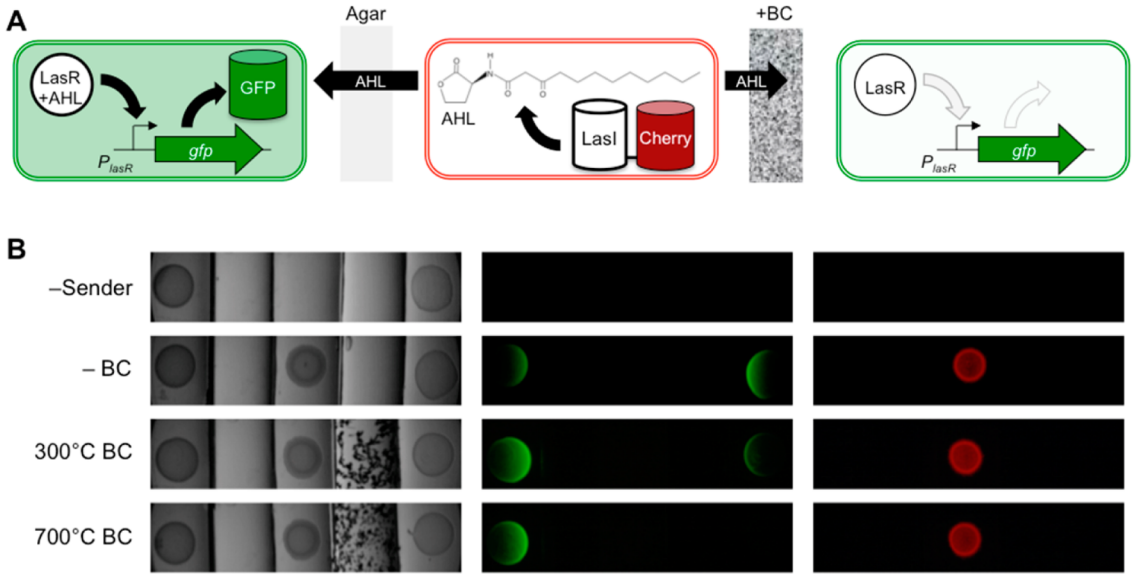

Figure 4. Biochars inhibit cell–cell communication to differing extents. (A) Agar plate assay for assessing biochar effects on *E. coli* sender–receiver communication. Sender cells were spotted between two agar slabs, one lacking biochar and one containing biochar materials (10 mg/mL). Receiver cells were spotted outside of both agar slabs. (B) Images of sender and receiver cells grown on agar plates containing identical amounts of 300 and 700 °C biochar materials within agar slabs. Bright field images (left) show cell growth, red fluorescence images (right) reveal constitutive expression of LasI-mCherry fusions in sender cells, and green fluorescence images (middle) illustrate how GFP protein expression varies in receiver cells. Biochar is designated BC in the figure.

extent to which microbes form and disperse organic matrices on soil surfaces[42,54] and could trigger agronomic effects by altering the fraction of microbes that infect plants and form soft rot.[55] Biochar interference with the intercellular signaling needed to trigger root infections may be an economically sought-after agronomic effect, and it may be possible to engineer biochars to intentionally trigger this interference. Alteration of biofilm formation may decrease or increase net CO_2 emissions, suggesting additional biochar engineering targets. Biochar amendment could also influence carbon fixation by altering signaling that nitrogen-fixing microbes use to establish and maintain symbiosis with plants,[42] which is critical in legumes for generating above ground biomass. A similar mechanism could underlie the recent observation that biochar and nutrient conditions exist under which mycorrhizal fungi switch from being mutualists of sorghum to being parasites.[25]

When preparing biochar, many parameters likely influence its ability to sorb biological molecules, including the feedstock, temperature, minerals, oxygen, and reactor type.[56,57] These parameters remain poorly constrained, limiting our ability to predict biochar properties upon amendment to soils. The microbial assay described here will be useful as a simple screen to characterize how these parameters influence biochar sorption of a single biological signaling molecule. Although the details of how biochar sorbs organic compounds are not completely understood, a number of studies indicate that the sorption of organics onto biochar is only partially reversible and can be saturated (as reviewed in Smernik[30]). This suggests that biochar's effects on microbial signaling should occur as a short-term pulse associated with the addition of fresh char into soils, and should decline as the char surface is saturated with organic molecules. Evidence exists that biochar particles become oxidized through both abiotic[58,59] and biotic[25] processes. Biochars also change adsorption capacity with simulated aging. Biochars can decrease in their capacity to absorb nonpolar molecules when they become loaded with lipids that block the access to interior pore networks,[60] and they can increase in ion exchange capacity.[61] Even if the observed sorption trends are transient within soils, short-lived biochar amendment effects within an ecosystem may be sufficient to drive changes in the trajectory of microbial community development, particularly if biochar is added at the time of seeding or seeding establishment. Charcoal from fires may have similar effects, as indicated by observations of short-term microbial impacts from natural charcoal on soil microbial processes.[23,62] Further analysis will be needed to determine if the biochar trends observed here are altered by weathering in the environment.

The experimental strategy described here illustrates how synthetic biology[63] can aid in constructing microbial assays to characterize the biological processes that drive complex ecological effects from biochar and other soil materials. Microbial biosensors will be useful for determining whether the trends we observe apply to the natural diversity of AHL used for quorum sensing, which have acyl chains of varying lengths,[43] as well as other classes of diffusible signaling molecules, such as those used for intraspecies[34,35] and interspecies[36,38] communication in bacteria (e.g., furanosyl borate diesters, indole, oligopeptides, and quinolones) and fungi (e.g., farnesol, tyrosol, and dimethoxycinnamate). For a given biochar, signaling molecule sorption is expected to vary from organism to organism because of differences in the structures of the molecules used for intercellular communication. Organisms using multiple signaling molecules for cell–cell communication may have only a subset of their intercellular conversations disrupted by a biochar. While our work focused on the effects of biochar on these intercellular conversations, the methods described here could also be used to test the single and combined effects of a wide range of soil materials on microbial communication, and our biochar results will ultimately benefit from being placed in this broad context.

A better understanding of biochar interactions with individual biochemical signals will help constrain parameter space in greenhouse experiments that seek to dissect the complex biotic

effects caused by biochar and require significant investments in time and space to achieve replication. Such information will be critical for anticipating the biological effects of soil biochar amendment and making land use decisions that maximize agricultural productivity and carbon sequestration while minimizing greenhouse gas emissions.

■ ASSOCIATED CONTENT

Supporting Information

Seven figures related to the concentration dependence of AHL-induced gene expression, biochar surface areas, cellular growth in the presence of AHL treated medium, charcoal sorption of AHL after different incubation times, methodology for creating agar plates, and biochar effects on cellular communication. This material is available free of charge via the Internet at http://pubs.acs.org.

■ AUTHOR INFORMATION

Corresponding Author

*(J.J.S.) Tel.: 713-348-3849. E-mail: joff@rice.edu. (C.A.M) Tel.: 713-348-5234. E-mail: masiello@rice.edu.

Notes

The authors declare no competing financial interest.

■ ACKNOWLEDGMENTS

We are grateful for financial support from the Hamill Foundation grant (to C.A.M., J.A.R., J.J.S., and K.Z.), Robert A. Welch Foundation Grants C-1614 (to J.J.S.) and C-1729 (to M.R.B.), National Science Foundation 0911685 (to C.A.M.), National Institute of Health R01GM104974 (to M.R.B.), as part of the joint NSF/NIGMS Mathematical Biology Program, and Taiwan Ministry of Education Scholarship (to H.Y.C.).

■ REFERENCES

(1) Masiello, C. A. New directions in black carbon organic geochemistry. *Mar. Chem.* **2004**, *92*, 201−213.

(2) Lehmann, J.; Gaunt, J.; Rondon, M. Bio-char sequestration in terrestrial ecosystems − A review. *Mitig. Adapt. Strat. Glob. Change* **2006**, *11*, 395−419.

(3) Major, J.; Rondon, M.; Molina, D.; Riha, S. J.; Lehmann, J. Maize yield and nutrition during 4 years after biochar application to a Colombian savanna oxisol. *Plant Soil* **2010**, *333*, 117−128.

(4) Zhang, A.; Liu, Y.; Pan, G.; Hussain, Q.; Li, L.; Zheng, J.; Zhang, X. Effect of biochar amendment on maize yield and greenhouse gas emissions from a soil organic carbon poor calcareous loamy soil from Central China Plain. *Plant Soil* **2011**, *351*, 263−275.

(5) Zhang, A.; Bian, R.; Pan, G.; Cui, L.; Hussain, Q.; Li, L. Effects of biochar amendment on soil quality, crop yield and greenhouse gas emission in a Chinese rice paddy: A field study of 2 consecutive rice growing cycles. *Field Crops Res.* **2012**, *127*, 153−160.

(6) Chan, K. Y.; Van Zwieten, L.; Meszaros, I.; Downie, A.; Joseph, S. Agronomic values of greenwaste biochar as a soil amendment. *Aust. J. Soil Res.* **2007**, *45*, 629.

(7) Kinney, T. J.; Masiello, C. A.; Dugan, B.; Hockaday, W. C.; Dean, M. R.; Zygourakis, K.; Barnes, R. T. Hydrologic properties of biochars produced at different temperatures. *Biomass Bioenergy* **2012**, *41*, 34−43.

(8) Briggs, C.; Breiner, J. M.; Graham, R. C. Physical and chemical properties of *Pinus ponderosa* charcoal. *Soil Science* **2012**, *177*, 263−268.

(9) Novak, J. M.; Busscher, W. J.; Watts, D. W.; Amonette, J. E.; Ippolito, J. A.; Lima, I. M.; Gaskin, J.; Das, K. C.; Stephen; Ahmedna, M.; Rehrah, D.; Schomberg, H. Biochars impact on soil-moisture storage in an ultisol and two aridisols. *Soil Science* **2012**, *177*, 310−320.

(10) Liu, J.; Schulz, H.; Brandl, S.; Miehtke, H.; Huwe, B.; Glaser, B. Short-term effect of biochar and compost on soil fertility and water status of a Dystric Cambisol in NE Germany under field conditions. *J. Plant Nutr. Soil Sci.* **2012**, *175*, 698−707.

(11) Elad, Y.; David, D. R.; Harel, Y. M.; Borenshtein, M.; Kalifa, H. B.; Silber, A.; Graber, E. R. Induction of systemic resistance in plants by biochar, a soil-applied carbon sequestering agent. *Phytopathology* **2010**, *100*, 913−921.

(12) Ventura, M.; Sorrenti, G.; Panzacchi, P.; George, E.; Tonon, G. Biochar reduces short-term nitrate leaching from a horizon in an apple orchard. *J. Environ. Qual.* **2013**, *42*, 76.

(13) Skjemstad, J. O.; Spouncer, L. R.; Cowie, B.; Swift, R. S. Calibration of the Rothamsted organic carbon turnover model (RothC ver. 26.3), using measurable soil organic carbon pools. *Aust. J. Soil Res.* **2004**, *42*, 79−88.

(14) Masiello, C. A. Black carbon in deep-sea sediments. *Science* **1998**, *280*, 1911−1913.

(15) Ziolkowski, L. A.; Druffel, E. Aged black carbon identified in marine dissolved organic carbon. *Geophys. Res. Lett.* **2010**, *37*, L16601.

(16) Kuzyakov, Y.; Subbotina, I.; Chen, H.; Bogomolova, I. Black carbon decomposition and incorporation into soil microbial biomass estimated by ^{14}C labeling. *Soil Biol. Biochem.* **2009**, *41*, 210−219.

(17) Santos, F.; Torn, M. S.; Bird, J. A. Biological degradation of pyrogenic organic matter in temperate forest soils. *Soil Biol. Biochem.* **2012**, *51*, 115−124.

(18) Singh, N.; Abiven, S.; Torn, M. S.; Schmidt, M. W. I. Fire-derived organic carbon in soil turns over on a centennial scale. *Biogeosciences* **2012**, *9*, 2847−2857.

(19) Zimmerman, A. R. Abiotic and microbial oxidation of laboratory-produced black carbon (biochar). *Environ. Sci. Technol.* **2010**, *44*, 1295−1301.

(20) Schmidt, M. W. I.; Torn, M. S.; Abiven, S.; Dittmar, T.; Guggenberger, G.; Janssens, I. A.; Kleber, M.; Kögel-Knabner, I.; Lehmann, J.; Manning, D. A. C.; Nannipieri, P.; Rasse, D. P.; Weiner, S.; Trumbore, S. E. Persistence of soil organic matter as an ecosystem property. *Nature* **2012**, *478*, 49−56.

(21) Wardle, D. A.; Nilsson, M.-C.; Zackrisson, O. Fire-derived charcoal causes loss of forest humus. *Science* **2008**, *320*, 629.

(22) Zimmerman, A. R.; Gao, B.; Ahn, M.-Y. Positive and negative carbon mineralization priming effects among a variety of biochar-amended soils. *Soil Biol. Biochem.* **2011**, *43*, 1169−1179.

(23) Mackenzie, M. D.; DeLuca, T. H. Charcoal and shrubs modify soil processes in ponderosa pine forests of western Montana. *Plant Soil* **2006**, *287*, 257−266.

(24) Dempster, D. N.; Gleeson, D. B.; Solaiman, Z. M.; Jones, D. L.; Murphy, D. V. Decreased soil microbial biomass and nitrogen mineralisation with Eucalyptus biochar addition to a coarse textured soil. *Plant Soil* **2011**, *354*, 311−324.

(25) LeCroy, C.; Masiello, C. A.; Rudgers, J. A.; Hockaday, W. C.; Silberg, J. J. Nitrogen, biochar, and mycorrhizae: Alteration of the symbiosis and oxidation of the char surface. *Soil Biol. Biochem.* **2013**, *58*, 248−254.

(26) Warnock, D. D.; Lehmann, J.; Kuyper, T. W.; Rillig, M. C. Mycorrhizal responses to biochar in soil—Concepts and mechanisms. *Plant Soil* **2007**, *300*, 9−20.

(27) Khodadad, C. L. M.; Zimmerman, A. R.; Green, S. J.; Uthandi, S.; Foster, J. S. Taxa-specific changes in soil microbial community composition induced by pyrogenic carbon amendments. *Soil Biol. Biochem.* **2011**, *43*, 385−392.

(28) Elad, Y.; Cytryn, E.; Harel, Y. M.; Lew, B.; Graber, E. R. The biochar effect: plant resistance to biotic stresses. *Phytopathol. Mediter.* **2012**, *50*, 335−349.

(29) Lehmann, J.; Rillig, M. C.; Thies, J.; Masiello, C. A.; Hockaday, W. C.; Crowley, D. Biochar effects on soil biota − A review. *Soil Biol. Biochem.* **2011**, *43*, 1812−1836.

(30) Smernik, R. J. Biochar and sorption of organic compounds. In *Biochar for Environmental Management: Science and Technology*; Lehmann, J., Joseph, S., Eds.; Science: London, 2009; pp 289−300.

(31) Spokas, K. A.; Koskinen, W. C.; Baker, J. M.; Reicosky, D. C. Impacts of woodchip biochar additions on greenhouse gas production

and sorption/degradation of two herbicides in a Minnesota soil. *Chemosphere* **2009**, *77*, 574−581.
(32) Beesley, L.; Moreno-Jiménez, E.; Gomez-Eyles, J. L. Effects of biochar and greenwaste compost amendments on mobility, bioavailability and toxicity of inorganic and organic contaminants in a multi-element polluted soil. *Environ. Pollut.* **2010**, *158*, 2282−2287.
(33) Zheng, W.; Guo, M.; Chow, T.; Bennett, D. N.; Rajagopalan, N. Sorption properties of greenwaste biochar for two triazine pesticides. *J. Hazard. Mater.* **2010**, *181*, 121−126.
(34) Ng, W.-L.; Bassler, B. L. Bacterial quorum-sensing network architectures. *Annu. Rev. Genet.* **2009**, *43*, 197−222.
(35) Hogan, D. A. Talking to themselves: Autoregulation and quorum sensing in fungi. *Eukaryotic Cell* **2006**, *5*, 613−619.
(36) Shaw, L. J.; Morris, P.; Hooker, J. E. Perception and modification of plant flavonoid signals by rhizosphere microorganisms. *Environ. Microbiol.* **2006**, *8*, 1867−1880.
(37) Oldroyd, G. E.; Downie, J. A. Coordinating nodule morphogenesis with rhizobial infection in legumes. *Annu. Rev. Plant Biol.* **2008**, *59*, 519−546.
(38) Lambrecht, M.; Okon, Y.; Vande Broek, A.; Vanderleyden, J. Indole-3-acetic acid: A reciprocal signalling molecule in bacteria-plant interactions. *Trends Microbiol.* **2000**, *8*, 298−300.
(39) DeAngelis, K. M.; Firestone, M. K.; Lindow, S. E. Sensitive whole-cell biosensor suitable for detecting a variety of N-acyl homoserine lactones in intact rhizosphere microbial communities. *Appl. Environ. Microbiol.* **2007**, *73*, 3724−3727.
(40) DeAngelis, K. M.; Lindow, S. E.; Firestone, M. K. Bacterial quorum sensing and nitrogen cycling in rhizosphere soil. *FEMS Microbiol. Ecol.* **2008**, *66*, 197−207.
(41) Basu, S.; Gerchman, Y.; Collins, C. H.; Arnold, F. H.; Weiss, R. A synthetic multicellular system for programmed pattern formation. *Nature* **2005**, *434*, 1130−1134.
(42) González, J. E.; Marketon, M. M. Quorum sensing in nitrogen-fixing rhizobia. *Microbiol. Mol. Biol. Rev.* **2003**, *67*, 574−592.
(43) Churchill, M. E. A.; Chen, L. Structural basis of acyl-homoserine lactone-dependent signaling. *Chem. Rev.* **2011**, *111*, 68−85.
(44) Wycuff, D. R.; Matthews, K. S. Generation of an AraC-araBAD promoter-regulated T7 expression system. *Anal. Biochem.* **2000**, *277*, 67−73.
(45) Gregg, S. J.; Sing, K. *Adsorption, Surface Area, and Porosity*; 2nd ed. Academic Press: London, 1983.
(46) Lutz, R.; Bujard, H. Independent and tight regulation of transcriptional units in *Escherichia coli* via the LacR/O, the TetR/O and AraC/I1-I2 regulatory elements. *Nucleic Acids Res.* **1997**, *25*, 1203−1210.
(47) Schneider, C. A.; Rasband, W. S.; Eliceiri, K. W. NIH Image to ImageJ: 25 years of image analysis. *Nat. Methods* **2012**, *9*, 671−675.
(48) Weissberg, H. L. Effective diffusion coefficient in porous media. *J. Appl. Phys.* **1963**, *34*, 2636.
(49) Pearson, J. P.; Gray, K. M.; Passador, L.; Tucker, K. D.; Eberhard, A.; Iglewski, B. H.; Greenberg, E. P. Structure of the autoinducer required for expression of *Pseudomonas aeruginosa* virulence genes. *Proc. Natl. Acad. Sci. U.S.A.* **1994**, *91*, 197−201.
(50) Charlton, T. S.; de Nys, R.; Netting, A.; Kumar, N.; Hentzer, M.; Givskov, M.; Kjelleberg, S. A novel and sensitive method for the quantification of N-3-oxoacyl homoserine lactones using gas chromatography−mass spectrometry: application to a model bacterial biofilm. *Environ. Microbiol.* **2000**, *2*, 530−541.
(51) Passador, L.; Cook, J. M.; Gambello, M. J.; Rust, L.; Iglewski, B. H. Expression of *Pseudomonas aeruginosa* virulence genes requires cell-to-cell communication. *Science* **1993**, *260*, 1127−1130.
(52) Decho, A. W.; Frey, R. L.; Ferry, J. L. Chemical challenges to bacterial AHL signaling in the environment. *Chem. Rev.* **2011**, *111*, 86−99.
(53) Rondon, M. A.; Lehmann, J.; Ramírez, J.; Hurtado, M. Biological nitrogen fixation by common beans (*Phaseolus vulgaris L.*) increases with bio-char additions. *Biol. Fertil. Soils* **2006**, *43*, 699−708.
(54) Karatan, E.; Watnick, P. Signals, regulatory networks, and materials that build and break bacterial biofilms. *Microbiol. Mol. Biol. Rev.* **2009**, *73*, 310−347.
(55) Dong, Y.-H.; Xu, J.-L.; Li, X.-Z.; Zhang, L.-H. AiiA, an enzyme that inactivates the acylhomoserine lactone quorum-sensing signal and attenuates the virulence of *Erwinia carotovora*. *Proc. Natl. Acad. Sci. U.S.A.* **2000**, *97*, 3526−3531.
(56) Masek, O.; Brownsort, P.; Cross, A.; Sohi, S. Influence of production conditions on the yield and environmental stability of biochar. *Fuel* **2013**, *103*, 151−155.
(57) Lin, Y.; Munroe, P.; Joseph, S.; Ziolkowski, A.; Van Zwieten, L.; Kimber, S.; Rust, J. Chemical and structural analysis of enhanced biochars: Thermally treated mixtures of biochar, chicken litter, clay and minerals. *Chemosphere* **2013**, *91*, 35−40.
(58) Nguyen, B. T.; Lehmann, J.; Kinyangi, J.; Smernik, R.; Riha, S. J.; Engelhard, M. H. Long-term black carbon dynamics in cultivated soil. *Biogeochemistry* **2008**, *92*, 163−176.
(59) Yao, F. X.; Arbestain, M. C.; Virgel, S.; Blanco, F.; Arostegui, J.; Maciá-Agulló, J. A.; Macías, F. Simulated geochemical weathering of a mineral ash-rich biochar in a modified Soxhlet reactor. *Chemosphere* **2010**, *80*, 724−732.
(60) Kwon, S.; Pignatello, J. J. Effect of natural organic substances on the surface and adsorptive properties of environmental black carbon (char): Pseudo pore blockage by model lipid components and its implications for N_2-probed surface properties of natural sorbents. *Environ. Sci. Technol.* **2005**, *39*, 7932−7939.
(61) Cheng, C.-H.; Lehmann, J.; Engelhard, M. H. Natural oxidation of black carbon in soils: Changes in molecular form and surface charge along a climosequence. *Geochim. Cosmochim. Acta* **2008**, *72*, 1598−1610.
(62) DeLuca, T. H.; Mackenzie, M. D.; Gundale, M. J.; Holben, W. E. Wildfire-produced charcoal directly influences nitrogen cycling in ponderosa pine forests. *Soil Sci. Soc. Am. J.* **2006**, *70*, 448−453.
(63) Slusarczyk, A. L.; Lin, A.; Weiss, R. Foundations for the design and implementation of synthetic genetic circuits. *Nat. Rev. Genet.* **2012**, *13*, 406−420.